






© The Author(s), 2024. Published by Cambridge University Press on behalf of University of Arizona. This is an Open Access article, distributed under the terms of the Creative Commons Attribution-NonCommercial-NoDerivatives licence (<http://creativecommons.org/licenses/by-nc-nd/4.0/>), which permits non-commercial re-use, distribution, and reproduction in any medium, provided that no alterations are made and the original article is properly cited. The written permission of Cambridge University Press must be obtained prior to any commercial use and/or adaptation of the article.

OPTICALLY STIMULATED LUMINESCENCE (OSL) MORTAR DATING INTER-COMPARISON STUDY. THE SECOND ROUND OF MODIS, MORTAR DATING INTER-COMPARISON STUDY

Petra Urbanová¹  • Laura Panzeri^{2*}  • Jorge Sanjurjo-Sánchez³  • Marco Martini² • Francesco Maspero²  • Pierre Guibert¹  • Anna Galli²

¹Archéosciences-Bordeaux UMR 6034, CNRS-Université Bordeaux Montaigne, Esplanade des Antilles, 33607 Pessac, France

²Dipartimento di Scienza dei Materiali, Università degli Studi di Milano-Bicocca, via R. Cozzi 55, 20125 Milano, Italy

³Instituto Universitario de Geología, Universidade da Coruña. ESCI, Campus de Elviña, 15017 A Coruña, Spain

ABSTRACT. After an intercomparison age experiment carried out in the framework of the first MODIS (Mortar Dating Inter-comparison Study) project, the results showed general agreement both between optically stimulated luminescence (OSL) dating laboratories and with radiocarbon (^{14}C) dating results. As the needs for the selection of samples convenient for an inter-comparison are not the same between ^{14}C and OSL, for the second running, it has been decided to choose two different sample sets, one to share between the radiocarbon labs and one for the OSL dating ones. The results obtained by applying different experimental protocols (multigrain and single grain techniques) and different statistical models (weighted mean, central age mode, average dose model, minimum age model and exponential exposure dose) are discussed in this work.

KEYWORDS: OSL, mortar dating, single grain.

INTRODUCTION

Mortars are among the most frequently used building materials from ancient times. Among the different kinds of traditional binders, lime mortars have historically been the most used worldwide. Contrary to what happens with other materials such as bricks or timber (Galli et al. 2020), mortars cannot be replaced without being destroyed, because of their mechanical properties. Thus, it is more suitable and much more representative for the chronology of buildings when compared to brick or wood constructions since it is made at the time of building.

They are thus a very good target material for dating ancient and historical buildings as they are contemporary to the process of building. That is why they have always attracted attention for dating. Two physical dating methods currently enable us to date binders: radiocarbon (^{14}C) dating and optically stimulated luminescence (OSL). The aim of the ^{14}C method is to date the moment of lime carbonation and so it applies to the binder component in lime-based mortars. On the other hand, OSL dating addresses the analysis of the aggregate, with the objective of determining the moment of its last exposure to light, prior to the embedding of the mortar within a built structure. Both methods underwent great progress in recent decades (Urbanová et al. 2020) thanks to the contribution of numerous research teams over Europe.

Early attempts to date mortar by radiocarbon started almost 60 years ago (Labeyrie and Delibrias 1964; Stuiver and Smith 1965), but a more systematic study on the problems and new

*Corresponding author. Email: laura.panzeri@unimib.it

methodological approaches were proposed and developed in the end of the 20th century, by Northern Europe research teams (Ringbom and Remmer 1995; Heinemeier et al. 1997) in the framework of the Mortar Dating Project (www.mortardating.com). At the beginning of the 21st Century, many other laboratories started to explore mortar dating with various methodological proposals (Nawrocka et al. 2005; Marzaioli et al. 2011; Hajdas et al. 2012; Hodgins et al. 2011; Michalska et al. 2013) which conducted to the first inter-comparison of protocols, initiated within the first MODIS (MOrtar Dating Inter-comparison Study) project.

The latter was set up at the Mortar dating workshop organized in April 2014 by the University of Padua (Italy). For the first time, specialists of luminescence dating were integrated into the mortar dating research group, in particular thanks to the scientific collaboration with the Swiss archaeologist S. Hueglin, running at that time between the research teams. Indeed, in the first two decades of the 21st century considerable progress was made also in the field of OSL dating of mortars (Urbanová et al. 2020).

Seven radiocarbon laboratories and two OSL laboratories participated in the first inter-comparison exercise (Hajdas et al. 2017; Hayen et al. 2017), in which the specific needs of the sample selection for luminescence dating have not been considered yet. When applying the OSL method, it is necessary to evaluate the environmental dose rate received by each sample. The context *in situ* from which mortar samples are extracted thus needs to be known when OSL dating is used, contrary to the ^{14}C method.

Following this first step, a new inter-comparison experiment called MODIS2 was set up in 2018 during the Mortar Dating International Meeting (Bordeaux, FR), organized by the research center Archéosciences-Bordeaux (ancient IRAMAT-CRP2A). As the needs for the selection of samples convenient for an inter-comparison are not the same between ^{14}C and OSL, it has been decided to choose two different sample sets, one to share between the radiocarbon labs (Artioli et al. forthcoming) and one for the OSL dating.

Three research groups specialized in luminescence dating participated in the intercomparison study: the University Institute of Geology at the University of A Coruña (Spain), the LAMBDA laboratory at the University of Milano-Bicocca and Archéosciences-Bordeaux at the University Bordeaux Montaigne. The goal of this paper is to discuss the results of this inter-laboratory experiment.

PRINCIPLES OF LUMINESCENCE DATING OF MORTARS

Radioactivity is ubiquitous in nature due to the presence of natural radionuclides, mostly U, Th and K radioisotopes in rocks and minerals (Aitken 1985). Quartz is the preferred dosimeter for luminescence dating, absorbing the energy released by ionizing radiation to which it has been exposed over time. Such energy leads to the emission of electrons which are subsequently trapped in crystalline lattice defects. Some defects situated deeper inside the lattice have a high thermal lifetime; these deep traps (stable traps associated with high energy levels) can adequately be used for dating. The total amount of trapped electrons within a crystal is proportional to the total energy absorbed and retained by the crystal (or dose), hence to the time it was exposed to radiation. As soon as the mineral is exposed to sunlight, trapped electrons absorb the photon energy and are released from the traps. Released electrons can recombine with other kinds of crystalline defects (*holes* reflecting electrons vacancies) with a consequent emission of light (the luminescence signal) which can be measured in the laboratory through heating for Thermoluminescence (TL) or through light stimulation for

OSL (Aitken 1985, 1998). The luminescence age is the ratio between the total absorbed radiation dose and the annual absorbed dose, where the numerator is estimated as equivalent dose (De or archaeological dose) and the denominator, Dr, is evaluated by determining the radiochemical composition (mainly U, Th and ^{40}K) of the sample and its environment. Note that in this paper, the term “De” means the dose measured for individual quartz aliquots or grains while the term “archeological dose” corresponds to the dose calculated by applying the different statistical methods to the measured series of De.

OSL dating of mortars is usually performed on the sand-sized quartz, present in the mortar aggregate (Panzeri 2013; Sanjurjo-Sánchez 2016; Panzeri 2019; Tirelli et al. 2020; Urbanová et al. 2020). As the OSL signal of quartz is bleached when grains are exposed to daylight, the OSL dating of mortar provides the time elapsed since its last exposure to light during mortar mixing and layering, which corresponds to the moment of the building construction. As the OSL method is applied to the aggregate, this technique can in principle be used not only on lime-based materials but also on other types of binders containing quartz or feldspars (for example in Panzeri et al. 2017 and Sanjurjo-Sánchez et al. 2020 it was used to date earthen mortar).

For OSL dating of mortars, two requirements are necessary to get a reliable result: the quartz grains have to provide an exploitable luminescence signal and all or at least a part of the studied grains has to show a sufficient bleaching degree (Urbanová et al. 2020). After some early attempts to date mortar with OSL, it was concluded that incomplete bleaching could be a widespread problem for dating mortars (Zacharias et al 2002; Goedicke 2003; Jain et al. 2004; Goedicke 2011). Indeed, in the case of partially bleached samples, the only way to attain a reliable archaeological dose is the use of the Single Grain analysis (SG; Duller et al 2000). This approach allows detecting the luminescence signal of each quartz grain individually, contrary to the multi-grain (MG) technique in which the OSL signal of a quartz aliquot containing from a hundred to a thousand grains is measured. The series of equivalent doses obtained through both SG and MG analyses are subsequently exploited by using statistical treatments specifically developed for OSL dating (Galbraith 1999; Thomsen 2007; Guerin 2017; Guibert 2017).

MORTAR SAMPLES

For the inter-comparison exercise, the goal was to provide materials of the known age which would exhibit various properties in terms of bleaching. At the same time, the mortar had to be available in a sufficient quantity so that it could be divided into several equal parts. The selection of the samples was performed in the framework of the interdisciplinary project MoDAq (Mortar dating in Aquitaine), funded by the Regional Council of Aquitania between 2016 and 2019. The project, coordinated by P. Guibert and executed by P. Urbanová, allowed having access and sampling authorizations to several emblematic early medieval religious monuments in the Aquitaine region (France) with a well-studied and dated stratigraphy. The archaeological sites involved within this experiment are *Saint-Jean Baptiste* chapel in Périgueux and *Notre-Dame de la Place* in Bordeaux. The detailed description of both sites and their stratigraphy are described in corresponding publications (Gaillard et al. 2015; Javel et al. 2019; Urbanová et al. 2022)

Mortar sample 1-BDX 17682 has been taken on the site *Saint-Jean Baptiste* chapel, in Périgueux (SE France, see Javel et al. 2019 for more details). It originates from the building

phase corresponding to the Roman habitation whose walls were later reused to construct a pentagonal apse. The reference date for this sample is the end of the 3rd century. It was deduced from the coins found in the layers associated with the construction of the Roman habitation which are contemporary to its occupation.

Mortar Samples 8-BDX 21216 and 16-BDX 21221 originate from the archaeological site located under the church *Notre-Dame de la Place*, in Bordeaux (SE France, see Urbanová et al. 2022 for the details). The first one, named 8-BDX 21216 comes from the remains of the Roman habitation, dated between the end of the 2nd century and the first half of the 4th century AD. Its reference date is based on the typo-chronological dating of ceramic fragments that were found during the excavation carried out in 1983 in the levels corresponding to the occupation of the habitation.

The second sample, 16-BDX 21221 originates from the foundations of the front facade of the early medieval church. For these wall remains, the reference date is based on both archaeological data and formal analyses of architecture. The construction of the church would start in the 10th century and would continue until the 12th century AD.

METHODS

EQUIVALENT DOSE (DE) DETERMINATION

Preparation of Samples

In order to obtain a pure quartz fraction, the following procedures were applied. The outer slice of the mortars was removed under subdued red light. The sand-sized grains (180–250 µm) were washed with water and treated with hydrochloric acid (37%) and hydrogen peroxide (10%) to remove carbonates and organic matter. Feldspars and heavy minerals were removed by density separation using sodium polytungstate solutions with densities of 2.62 g/cm³ and 2.70 g/cm³.

In the cases of Milano and A Coruña, the remaining quartz fraction was etched in concentrated hydrofluoric acid (40%) to remove any remaining feldspars and the alpha-influenced outer portion of the grain.

In Bordeaux, the quartz fraction was etched with the mixture of the hexafluorosilicic and nitric acid in the ratio of 9:1, that shows high efficacy to remove feldspars without any risk of uneven etching of quartz grains (Urbanová et al. 2015). The alpha contribution to the annual dose was considered using a k-value equal to 0.05 ± 0.02 (Blain et al. 2007; Guibert et al. 2009).

In all three laboratories, the last step of the chemical treatment consisted in the second etching of the quartz fraction with hydrochloric acid (10%) to remove any potentially present soluble fluorides. Then the grains were dried. A total dissolution of feldspar in the etched quartz fractions was verified before starting the dating procedure by infrared stimulation (IRSL) test.

Experimental Setups

To determine De, all laboratories used Automated Risoe TL/OSL system readers for luminescence measurements. The reader is equipped with blue light-emitting diodes (LEDs, 470 nm) for MG measurements and a 10 mW Nd:YVO₄ solid-state diode-pumped laser emitting at 532 nm for SG analysis. The signals are recorded with a 9235QA photomultiplier

tube (PMT) coupled with a Hoya U-340 filter. Laboratory doses were given using a $^{90}\text{Sr}/^{90}\text{Y}$ beta source (dose rate at the time of measurement: $0.10 \pm 0.01 \text{ Gy s}^{-1}$ A Coruña lab; $0.11 \pm 0.03 \text{ Gy s}^{-1}$ Milano lab, and $0.13 \pm 0.01 \text{ Gy s}^{-1}$ for Bordeaux lab).

For the MG technique, the sample was mounted on stainless steel discs; for the Coruna lab each MG aliquot contains about one hundred grains while for the Milano labs about one thousand grains. For the SG procedure, quartz grains were mounted on special aluminum disks (10 mm diameter) with a grid of 10 x 10 holes holding the crystals.

The SAR (single aliquot regenerative; Murray and Wintle 2000) protocol was used in order to determine the De. The OSL was stimulated for 40 s at 125°C for MG measurements. Individual De values were accepted if the following criteria occurred: recycling ratio between 0.9 and 1.1, recuperation < 5%, IR signal < 5%. In the case of SG measurements, the grains were rejected if one of the following conditions was not satisfied: the signal was less than 3 standard deviations above the background, the recycling ratio was out of the 0.75–1.25 range, the error associated with the test dose was >25%, the signal of the natural De is out of the range of the laboratory regeneration doses. The preheat value was experimentally derived on the basis of the results of a dose recovery preheat plateau test (Wintle and Murray 2006).

DOSE RATE DETERMINATION

To measure the ^{40}K content, the Laboratory of A Coruña employed X-ray fluorescence spectrometry. A Bruker-Nonius S4 Pioneer wavelength dispersive fluorescence spectrometer under helium purge was used for this purpose. The U and Th radioisotope contents were estimated by Inductively Coupled Plasma Mass Spectrometry (ICP-MS). The analyses were carried out in a Thermo Scientific™ ELEMENT XR™ ICP-MS that combines a dual-mode SEM with a Faraday detector. Lithium metaborate fusion was used for sample preparation.

In the Milano Laboratory, ^{238}U and ^{232}Th concentrations were obtained by alpha counting by using ZnS scintillator discs and assuming Th/U concentration ratio equal to 3 (Aitken 1985). The contribution due to ^{40}K content was obtained from the total concentration of K measured by flame photometry.

In case of Bordeaux, a low background gamma spectrometer with a U-shape well Ge detector (Eurisys Mesures, EGPC 200 P17), whose active volume is 200 cm^3 and the well dimensions are 17 mm in diameter and 50 mm in depth was used to measure K, U and Th contents on homogenized powdered mortar samples in gamma spectrometry containers. The duration of counting varied from 3 to 7 days depending on the sample activity. The energy window of interest lies between 40 keV (^{210}Pb at 46.7 keV) and 2700 keV (^{208}Tl at 2614.5 keV).

All obtained radiochemical data were converted into the related dose rates using the conversion factors published by Guérin et al. (2011) in order to determine the sample matrix contributions to α and β dose rates. Dose attenuation coefficients of α and β dose rates in coarse grains were calculated according to Bell (1979) and Brennan et al. (1991).

The contributions of gamma and cosmic dose rates were evaluated using in situ dosimetry. The dosimeters were left *in situ* at the precise location where the mortars for dating were taken. The effects of radioactivity accumulated by the $\text{Al}_2\text{O}_3:\text{C}$ pellets contained within the dosimeters were measured with a *lexsyg* SMART luminescence reader (Kreutzer et al. 2018), equipped with a calibrated $^{90}\text{Sr}/^{90}\text{Y}$ beta source. Additional measurements by on site gamma

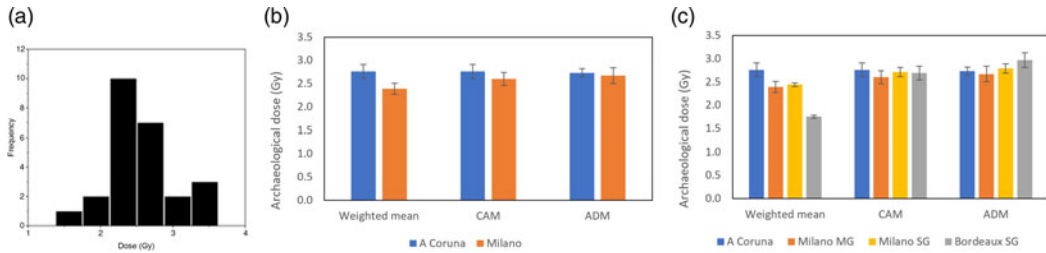


Figure 1 (a) Distribution of D_e obtained by Milano lab on sample 1-BDX 17682 with MG technique. (b) Archaeological dose obtained with MG technique calculated with different statistical models on sample 1-BDX 17682 by A Coruña and Milano labs. The weight in the weighted mean was calculated as $1/(\sigma_i)^2$ where σ_i is the error of each D_e . (c) Archaeological dose obtained applying MG and SG techniques with different age models on sample 1-BDX 17682.

spectrometry, using a portable Canberra NaI:Tl (1.5" × 1.5") Inspector system were undertaken and provided the results in agreement with the data acquired by dosimetry.

The saturation water content of the studied mortar samples ranged from 10 to 20 %. A value of $75 \pm 15\%$ of saturation was assumed for all dose rate calculations. This value takes into account the water content of the samples immediately after sampling and the fact that the mortars were buried for one thousand years.

RESULTS

Archeological Dose Evaluation

The results of the OSL measurements, allowing to measure the D_e distributions for individual samples and consequently to calculate the archaeological dose, are presented in the following paragraph. While in A Coruña all OSL measurements were performed with the MG technique, the Bordeaux lab employed exclusively the SG procedure. The Milano lab carried out systematically both the SG and the MG analyses.

First of all, the results obtained with the MG technique will be discussed. Sample 1-BDX 17682 exhibits complete bleaching, as indicated by the Gaussian distribution of the D_e (see Figure 1a). In order to provide the comparison of different existing models convenient for the well bleached samples, the weighted mean, the CAM (central age model; Galbraith et al. 1999) and the ADM (average dose model; Guérin et al. 2017) were used for archaeological dose evaluation. All these models are suitable exclusively for the well-bleached samples, providing normal or log-normal distribution of D_e .

All the results obtained show a very good agreement within one standard error (Figure 1b). In fact, comparing MG archaeological doses obtained by the labs of A Coruña and Milano, there are no significant differences. The results obtained on SG aliquots on the well bleached sample 1-BDX 17682 are compatible with MG D_e , except for the weighted mean of Bordeaux lab (see Figure 1c).

Mortar samples 8-BDX 21216 and 16-BDX 21221 are instead affected by incomplete bleaching. The MG distributions of the D_e are widely scattered as shown in Figure 2a and 2b. Indeed, the SG measurements showed that an important proportion of the well bleached grains

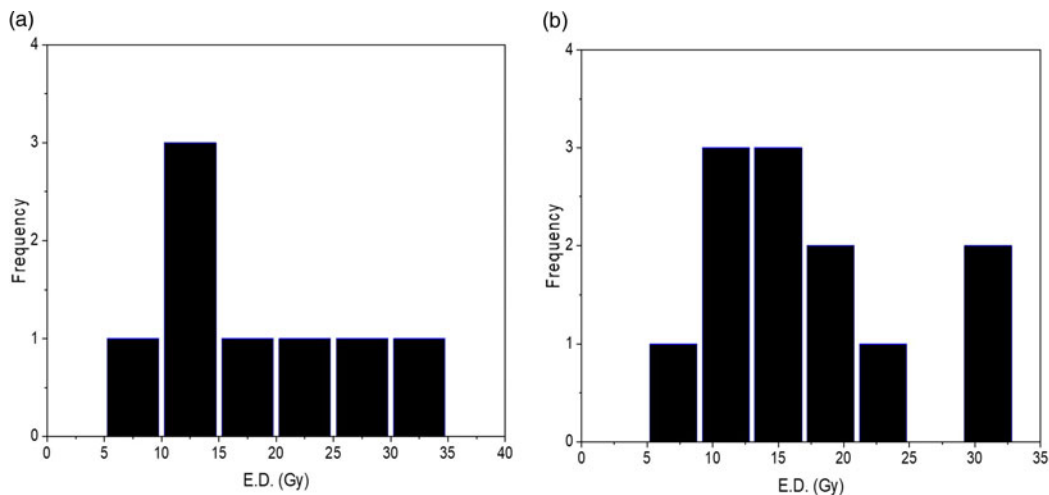


Figure 2 MG De distribution for samples 8-BDX 21216 (a) and 16-BDX 21221 (b) obtained by Milano Lab.

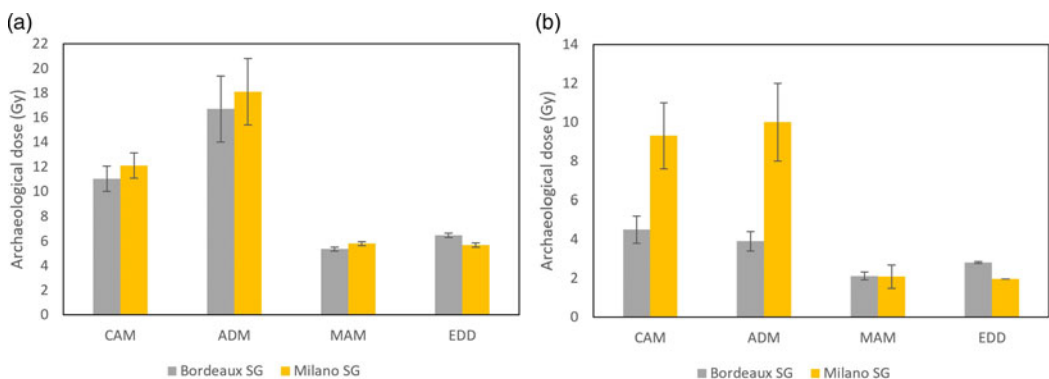


Figure 3 Archaeological dose obtained applying SG technique with different age models on samples (a) 8-BDX 17862 and (b) 16-BDX 21221. The MAM3 was applied using an intrinsic over-dispersion parameter (OD) determined by a dose recovery test. Number of acceptable grain/measured grains: sample 8-BDX 21216: 99/ 6175, 1.6 % (Bordeaux), 63/4000; 1.6% (Milano); sample 16-BDX 21221: 127/3420; 2.7 % (Bordeaux), 79/2000; 3.9% (Milano).

is present in the distributions, which are, however, characterized by a long tail towards higher doses, indicating a non-negligible presence of partially bleached grains. Therefore, the CAM and the ADM dose models cannot logically provide a reliable estimation of the archeological dose, contrary to the MAM (minimum age model; Galbraith 1999) and EED (exponential exposure dose; Guibert et al. 2017).

The results obtained by Milano and Bordeaux labs are reported in Figure 3. The archeological doses resulting from the use of CAM and ADM are significantly higher than those calculated with MAM and EED. As reported in the caption of Figure 3 the number of acceptable versus analyzed grains is around 1–4% that in the experience of the authors it is not a low percentage for mortar samples.

Table 1 U, Th, and K₂O content of the mortar samples determined by the three laboratories.

	Lab	U (ppm)	Th (ppm)	K ₂ O (weight%)	Dose rate (Gy/ka)
1-BDX 17682	A Coruña	1.45 ± 0.07	5.9 ± 0.3	1.10 ± 0.01	1.49 ± 0.08
	Milano	2.05 ± 0.10	6.5 ± 0.3	0.67 ± 0.02	1.54 ± 0.08
	Bordeaux	1.79 ± 0.13	5.25 ± 0.08	1.08 ± 0.02	1.88 ± 0.11
8-BDX21216	A Coruña	10.0 ± 0.5	2.14 ± 0.11	0.84 ± 0.01	2.24 ± 0.08
	Milano	12.1 ± 0.6	38 ± 2	0.67 ± 0.02	3.40 ± 0.17
	Bordeaux ⁽¹⁾	21.8 ± 0.6	2.55 ± 0.10	1.03 ± 0.02	3.78 ± 0.16
16-BDX21221	A Coruña	2.46 ± 0.12	2.49 ± 0.12	0.71 ± 0.01	1.31 ± 0.08
	Milano	3.21 ± 0.16	10.14 ± 0.13	0.66 ± 0.02	1.89 ± 0.10
	Bordeaux ⁽²⁾	2.57 ± 0.12	2.47 ± 0.06	1.00 ± 0.02	1.85 ± 0.05

⁽¹⁾U238: 21.8 ± 0.6 ppm; Ra226: 17.5 ± 0.2 ppm; Pb210: 20.0 ± 2.0 ppm.

⁽²⁾U238: 2.57 ± 0.12 ppm; Ra226: 2.25 ± 0.03 ppm; Pb210: 2.4 ± 0.3 ppm.

Dose Rate Evaluation

For the evaluation of the dose rate, all three laboratories considered the same value of water content and of environmental dose rate, as both parameters were determined through *in situ* analyses at the moment of sampling. The differences in the dose rate thus originate exclusively from the quantification of radioelement contents within the sample matrix.

The U, Th, and ⁴⁰K contents determined for sample 1-BDX 17682 were comparable within one standard error for all three labs. The U contents determined for samples 8-BDX 21216 and 16-BDX21221 by different participants show high variability (see table 1). Two possible explanations may be suggested. In the case of samples 8-BDX 21216, the low background gamma spectrometry analyses performed in Bordeaux showed the presence of slight disequilibrium in the Uranium decay chains that cannot be detected by the methods employed by Milano and Coruna (the data are reported in the caption of Table 1). Nevertheless, the dose rate calculated for two “extreme” situations (the first one for the recent mobility of Radon, the second for the ancient and continuous mobility of Radon) and the final dose rate was very close one to each other. As for the Th content determined by the Milano group, we note a large overestimation. In fact, the value was not measured but it was deduced from the U/Th ratio of 3, typical to ceramics, which is obviously not adapted for mortar composition. Another argument that can partly explain the variations observed in radioelement contents of the sample 8-BDX 21216 is its high microdosimetric heterogeneity caused by inhomogeneous distribution of radioactive elements within the sample matrix.

To conclude, while there are no significant differences in the dose rate estimated for sample 1-BDX 17682, we detect significant variations for the other samples. The difference in the total dose rate for sample 8-BDX 21216 is around 30% between the laboratory of A Coruña and the other laboratories. For sample 16-BDX 21221 the difference is similar between the laboratory of A Coruña and the laboratory of Bordeaux and around 10% for the laboratories of Bordeaux and Milano.

DISCUSSION

As it can be expected in mortar dating, the main critical aspect in the archaeological dose evaluation is the incomplete and/or heterogeneous zeroing of the OSL signal after the sunlight

exposure of quartz grains during mortar mixing and layering. At first glance, if the distribution of equivalent doses measured on multigrain aliquots is normal or log-normal, then it is likely that the quartz grains were all completely zeroed. This is observed in the behavior of sample 1-BDX 17682 (Figure 1a), confirmed also by the convergence of all the analytical and statistical methods applied (Figure 1c). The calculated ages for both MG and SG are consistent with the expected one within errors, with the exception of the result on SG archaeological dose obtained with CAM model by the Bordeaux lab. This date is a bit younger with respect to the expected age: the lab has dated other mortars and sediments from the same building phase and the Chi-squared test did not reveal any significant statistical divergence with other dating if the uncertainty is considered.

For the samples which are affected by heterogeneous or incomplete bleaching, the intercomparison confirms that the use of the SG technique is recommended. As expected, and largely demonstrated in the past, for the poorly bleached samples such as 8-BDX 21216 and 16-BDX 21221, the statistical models as CAM and ADM are not adapted. Their use provokes a dose over-estimation, as showed in Figure 3. Instead, the application of the MAM and the EED allows to overcome the problems of heterogeneous bleaching and determine the trustworthy archeological dose. As it is possible to observe in Figures 4, for the samples 8-BDX21216 and 16-BDX21221, there is an agreement between the experimental ages and the reference ones. SG De distributions are typically characterized by greater amounts of scattering in comparison to MG due to the low signal-to-noise ratios of the measured decay curves. The SAR De calculations were characterized by very large uncertainties that are reflected in the width of the age distributions.

As for the other critical aspect in the age calculation for mortar samples, the dose rate evaluation, the environmental dose rate to each grain per annum is a combination of internal and external sources of alpha and beta particles and external gamma and cosmic rays. Internal dose rates have been determined from bulk samples taken from the mortars and the material is powdered prior to measurements to homogenize it. In contrast, De values are determined from individual quartz grains from a sub-sample of the bulk material. Thus, the bulk estimation of the annual dose rate cannot quantify or account for any microscale heterogeneity in the annual dose rate to individual grains dispersed in the bulk material. This is the case of the 8-BDX21216 sample, which shows the U and Th disequilibrium also.

To evaluate the disequilibrium, the concentration of both U and Th contents need to be measured directly, instead of deducing Th content from the U content. The equilibrium conditions between mother and daughter isotopes for ^{238}U and ^{232}Th decay chains is also to be systematically checked.

For the micro dosimetry issue, etching to remove the surface of the quartz grains by hydrofluoric acid during sample preparation removes the alpha-influenced outer portion of the grain, while the effective ranges of gamma and cosmic rays extend far beyond the volume of a typical OSL sample taken in the field or an individual quartz grain (180-250 μm in diameter). Moreover, studies have shown that the internal alpha and beta dose rates arising from U and Th inclusions within a quartz grain are negligible (e.g. Jacobs et al. 2006). Thus, it is only the external beta dose rate arising from either K, Rb, U, and Th that could cause microscale heterogeneities in the dose rate, where beta particles are deposited as a nonlinear function of distance from the point source (e.g. a K-feldspar or zircon grain). Burbidge et al. (2009) established that U and Th, and hence internal α activity, were spatially associated with the presence of Fe, which was identified along structural defects in quartz crystals. They suggested

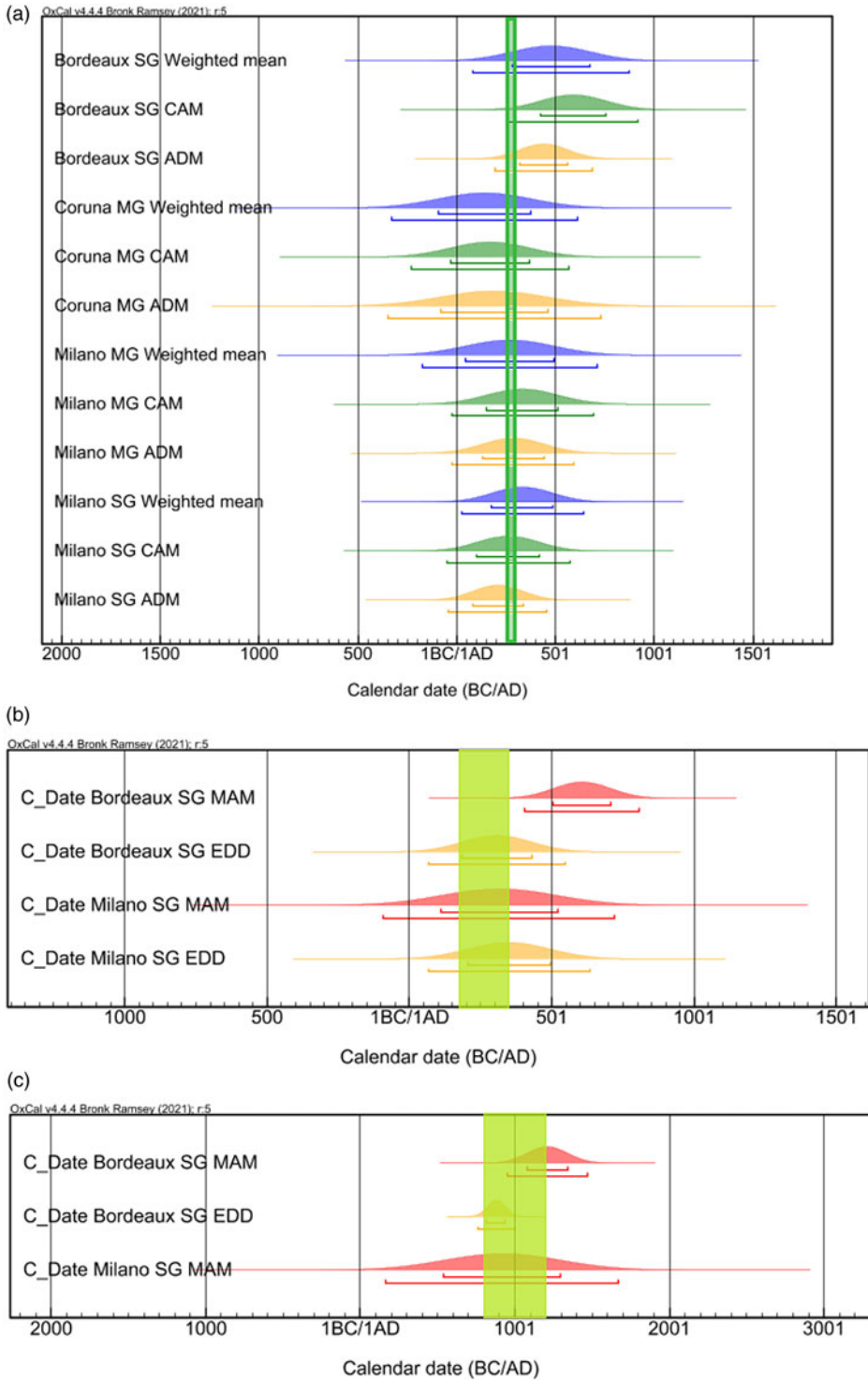


Figure 4 Probability density curves of the mortar samples obtained by the three laboratories using different statistical models and OSL protocols to determine the archaeological doses. The expected ages are indicated with a green bar. (a) Sample 1-BDX-17682; (b) Sample 8-BDX21216; (c) Sample 16-BDX212.

to remove the most affected grains by magnetic separation. Smedley et al. (2020) in their work suggested that it is possible to infer the relative standard deviation of the beta-dose heterogeneity for each sample using just the beta dose-rate, instead of acquiring empirical data for every sample. By analyzing a very large set of samples, they deduce how to determine accurate OSL ages and prevent underestimation of the burial ages. This suggestion is a possible answer to overcome the microdosimetry issue for the mortar samples also.

It can be said that microdosimetric heterogeneity provokes scatter at the main part of the distribution (Guérin et al. (2015) and Mayya et al. (2006)) and doesn't contribute to high De. These last are instead caused by the partial bleaching.

CONCLUSIONS

Despite all the highlighted problems arising from partial bleaching, disequilibrium and microdosimetry effects, obtained ages are consistent with the expected ones. From the experience of this inter-comparison, it is convenient to proceed with the MG approach as the first step. If the distribution of equivalent doses measured is normal or log-normal, then it is likely that the quartz grains were all completely zeroed at the same time and the calculated age will be affordable independently by statistical model applied. If the distribution of equivalent doses indicates incomplete bleaching, the MAM and the EED statistical analyses on equivalent doses measured on SG aliquots provide the results which are the most consistent with the expected ages. For both analytical techniques, MG and SG, when the dose rate is evaluated, the distribution of radioactive elements within the sample matrix has to be considered.

REFERENCES

- Aitken MJ. 1985. Thermoluminescence dating. London: Academic Press.
- Aitken MJ. 1998. An introduction to optical dating. Oxford University Press.
- Artioli G, Barone S, Fedi M, Galli A, Liccioli L, Martini M, Marzaioli F, Maspero F, Panzeri L, Passariello I, Ricci G, Secco M, Terrasi F. Forthcoming. Characterization and selection of mortar samples for radiocarbon dating in the framework of the MODIS2 intercomparison: two compared procedures. Radiocarbon.
- Bell WT. 1979. Attenuation factors to absorbed dose in quartz inclusions for thermoluminescence dating. *Ancient TL* 8:2–13.
- Blain S, Guibert P, Bouvier A, Vieilleveigne E, Bechtel F, Sapin C, Baylé M. 2007. TL-dating applied to building archaeology: The case of the medieval church Notre-Dame-Sous-Terre (Mont-Saint Michel, France). *Radiation Measurements* 42:1483–1491.
- Brennan BJ, Lyons RG, Phillips SW. 1991. Attenuation of alpha particle track dose for spherical grains. *Radiation Measurement* 18:249–253.
- Burbidge CI, Dias MI, Prudêncio MI, Rebêlo LP, Cardoso G, Brito P. 2009. Internal α activity: localisation, compositional associations and effects on OSL signals in quartz approaching β saturation. *Radiation Measurements* 44:494–500.
- Duller GAT, Bøtter-Jensen L, Murray AS. 2000. Optical dating of single sand-sized grains of quartz: sources of variability. *Radiation Measurements* 32:453–457.
- Gaillard H. 2015. Un nouvel élément dans la topographie chrétienne de Périgueux: la chapelle Saint-Jean-Baptiste à la Cité, in *Les sarcophages de l'Antiquité tardive et du haut Moyen Âge: fabrication, utilisation, diffusion*, Actes des XXXe Journées internationales d'archéologie mérovingienne (Bordeaux, 2–4 October 2009). Cartron I, Henrion F, Scuiller C, editors. p. 549–565.
- Galbraith RF, Roberts RG, Laslett GM, Yoshida H, Olley JM. 1999. Optical dating of single and multiple grains of quartz from Jinnium Rock Shelter, northern Australia: Part I, experimental design and statistical models. *Archaeometry* 41(2):339–364.
- Galli A, Sibilia E, Martini M. 2020. Ceramic chronology by luminescence dating: how and when it is possible to date ceramic artifacts. *Archaeological Anthropologica Science* 12:190.
- Goedicke C. 2003. Dating historical calcite mortar by blue OSL: results from known age samples. *Radiation Measurements* 37:409–415.
- Goedicke C. 2011. Dating mortar by optically stimulated luminescence: a feasibility study. *Geochronometria* 38(1):42–49.

- Guérin G, Christophe C, Philippe A, Murray A, Thomsen K, Tribolo C, Urbanova P, Jain M, Guibert P, Mercier N. 2017. Absorbed dose, equivalent dose, measured dose rates, and implications for OSL age estimates: Introducing the average dose model. *Quaternary Geochronology* 41:163–173.
- Guérin G, Mercier N, Adamiec G. 2011. Dose-rate conversion factors: update. *Ancient TL* 29:5–8.
- Guérin G, Myank J, Thomsen K, Murray A, Mercier N. 2015. Modelling dose rate to single grains of quartz in well-sorted sand samples: the dispersion arising from the presence of potassium feldspars and implications for single grain OSL dating. *Quaternary Geochronology* 27:52–65.
- Guibert P, Bailiff IK, Blain S, Gueli AM, Martini M, Sibilia E, Stella G, Troja S. 2009. Luminescence dating of architectural ceramics from an early medieval abbey: the St-Philbert intercomparison (Loire Atlantique, France). *Radiation Measurements* 44:488–493.
- Guibert P, Christophe C, Urbanova P, Guérin G, Blain S. 2017. Modeling incomplete and heterogeneous bleaching of mobile grains partially exposed to the light: towards a new tool for single grain OSL dating of poorly bleached mortars. *Radiation Measurements* 107:48–57.
- Hajdas I, Lindroos A, Heinemeier J, Ringbom A, Marzaioli F, Terrasi F, Passariello I, Capano M, Artioli G, Addis A, et al. 2017. Preparation and dating of mortar samples—Mortar Dating Inter-Comparison Study (MODIS). *Radiocarbon* 59: 1845–1858.
- Hajdas I, Trumm J, Bonani G, Biechele C, Maurer M, Wacker L. 2012. Roman ruins as an experiment for radiocarbon dating of mortar. *Radiocarbon* 54(3–4):897–903.
- Hayen R, VanStrydonck M, Fontaine L, Boudin M, Lindroos A, Heinemeier J, Ringbom Å, Michalska D, Hajdas I, Hueglin S, et al. 2017. Mortar dating methodology: Assessing recurrent issues and needs for further research. *Radiocarbon* 59(6): 1859–1871.
- Heinemeier J, Jungner H, Lindroos A, Ringbom Å, von Konow T, Rud N. 1997. AMS ^{14}C dating of lime mortar. *Nuclear Instruments and Methods in Physics Research B* 123(1–4):487–495.
- Hodgins G, Lindroos A, Ringbom Å, Heinemeier J, Brock F. 2011. ^{14}C dating of Roman mortars—preliminary tests using diluted hydrochloric acid injected in batches. *Commentationes Humanarum Litterarum* 128:209–13.
- Jacobs Z, Duller GAT, Wintle AG. 2006. Interpretation of single-grain De distributions and calculation of De. *Radiation Measurement* 41:264–277.
- Jain M, Thomsen KJ, Bøtter-Jensen L, Murray AS. 2004. Thermal transfer and apparent-dose distributions in poorly bleached mortar samples: results from single grains and small aliquots of quartz. *Radiation Measurements* 38:101–109.
- Javel JB, Urbanová P, Guibert P, Gaillard H. 2019. Chronological study of the Saint Jean-Baptiste chapel, Périgueux, France: contributions of mortar luminescence dating to history of local Christianity. *Archeologia dell'Architettura* XXIV:97–114.
- Kreutzer S, Martin L, Guérin G, Tribolo C, Selva P, Mercier N. 2018. Environmental dose rate determination using a passive dosimeter: techniques and workflow for $\alpha\text{-Al } 2\text{O}_3\text{:C}$ chips. *Geochronometria* 45(1):56–67.
- Labeurie J, Delibrias G. 1964. Dating of old mortars by the carbon-14 method. *Nature* 201:742.
- Marzaioli F, Lubritto C, Nonni S, Passariello I, Capano M, Terrasi F. 2011. Mortar radiocarbon dating: preliminary accuracy evaluation of a novel methodology. *Analytical Chemistry* 83(6):2038–2045.
- Mayya YS, Morthekai P, Murari MK, Singhvi AK. 2006. Towards quantifying beta microdosimetric effects in single-grain quartz dose distribution. *Radiation Measurements* 41:1032–1039.
- Michalska D, Pazdur A, Czernik J, Szczepaniak M, Żurakowska M. 2013. Cretaceous aggregate and reservoir effect in dating of binding materials. *Geochronometria* 40(1):33–41.
- Murray AS, Wintle A. 2000. Luminescence dating of quartz using an improved single-aliquot regenerative dose protocol. *Radiation Measurements* 32:523–538.
- Nawrocka D, Michniewicz J, Pawlyta J, Pazdur A. 2005. Application of radiocarbon method for dating of lime mortars. *Geochronometria* 24:109–115.
- Panzeri L. 2013. Mortar and surface dating with optically stimulated luminescence (OSL): Innovative techniques for the age determination of buildings. *Nuovo Cimento C* 36C:205–216.
- Panzeri L, Cantù M, Martini M, Sibilia E. 2017. Application of different protocols and age-models in OSL dating of earthen mortars. *Geochronometria* 44(1):341–351.
- Panzeri L, Caroselli M, Galli A, Lugli S, Martini M, Sibilia E. 2019. Mortar OSL and brick TL dating: the case study of the UNESCO World Heritage Site of Modena. *Quaternary Geochronology* 49:236–241.
- Ringbom Å, Remmer C. 1995. Ålands kyrkor, Volym I, Hammarland och Eckerö. *Naturvetenskaplig datering*. Mariehamn. p. 60–68.
- Sanjurjo-Sánchez J. 2016. Dating historical buildings: an update on the possibilities of absolute dating methods. *International Journal of Architectural Heritage* 10:620–635.
- Sanjurjo-Sánchez J, Blanco-Rotea R, García Quintela MV, Burbidge CI. 2020. OSL dating of earthen mortars from a medieval building in north-western Spain: Crypt of Basilica da Ascensión (Allariz, Ourense). *Radiocarbon* 62:679–692.

- Smedley R, Duller G, Rufer D, Utley J. 2020. Empirical assessment of beta dose heterogeneity in sediments: Implications for luminescence dating. *Quaternary Geochronology* 56:101052.
- Thomsen KJ, Murray AS, Bøtter-Jensen L, Kinahan J. 2007. Determination of burial dose in incompletely bleached fluvial samples using single grains of quartz. *Radiation Measurements* 42:370–379.
- Tirelli G, Lugli S, Galli A, Hajdas I, Lindroos A, Martini M, Maspero F, Olsen J, Ringbom Å, Sibilía E, Caroselli M, Silvestri E, Panzeri L. 2020. Integrated dating of the construction and restoration of the Modena cathedral vaults (Northern Italy): preliminary results. *Radiocarbon* 62(3):667–677.
- Stuiver M, Smith CS. 1965. 6th International Conference on Radiocarbon and Tritium Dating, Pullman, WA. p. 338–343.
- Urbanová P, Boaretto E, Artioli G. 2020. The state-of-the-art of dating techniques applied to ancient mortars and binders: a review. *Radiocarbon* 62(3):503–525.
- Urbanová P, Hourcade D, Ney C, Guibert P. 2015. Sources of uncertainties in OSL dating of archaeological mortars: the case study of the Roman amphitheatre Palais-Gallien in Bordeaux. *Radiation Measurements* 72:100–110.
- Urbanová P, Régado-Saint Blancard P, Guibert P, Lanos P, Hervé G, Dufresne P, Bouvier A. 2022. Le site paléochrétien Notre-Dame de la Place à Bordeaux : nouveaux acquis chronologiques. *Archéologie Médiévale*.
- Wintle A, Murray AS. 2006. A review of quartz optically stimulated luminescence characteristics and their relevance in single-aliquot regeneration dating protocols. *Radiation Measurements* 41:369–339.
- Zacharias N, Mauz B, Michael CT. 2002. Luminescence quartz dating of lime mortars. A first research approach. *Radiation Protection Dosimetry* 101(1–4):379–382.